Hindawi
International Journal of Photoenergy
Volume 2020, Article ID 8893816, 9 pages
https://doi.org/10.1155/2020/8893816

Research Article

Effects of Initial Nitrate Concentrations and Photocatalyst Dosages on Ammonium Ion in Synthetic Wastewater Treated by Photocatalytic Reduction

Orawan Rojviroon[1], **Sanya Sirivithayapakorn**[1], **Thammasak Rojviroon**[2] and **Chalermraj Wantawin**[1]

[1]*Department of Environmental Engineering, Faculty of Engineering, Kasetsart University, Bangkok 10900, Thailand*
[2]*Division of Environmental Engineering, Faculty of Engineering, Rajamangala University of Technology Thanyaburi, Pathum Thani 12110, Thailand*

Correspondence should be addressed to Sanya Sirivithayapakorn; fengsys@ku.ac.th

Received 6 August 2020; Revised 16 October 2020; Accepted 24 October 2020; Published 16 November 2020

Academic Editor: Jiangwei LIU

Ammonium (NH_4^+) is an undesirable by-product of photocatalytic nitrate (NO_3^-) reduction since it is harmful to aquatic life once it converts into ammonia (NH_3). This research investigated the removal efficiency of NO_3^- and for the first time quantified the relationships of initial nitrate concentrations ($[NO_3^-]_0$) and photocatalyst dosages on the remaining ammonium (NH_4^+) in synthetic wastewater using photocatalytic reduction process with either nanoparticle titanium dioxide (TiO_2) or 1.0%Ag-TiO_2 under Ultraviolet A (UVA). The experiments were systematically carried out under various combinations of $[NO_3^-]_0$ (10, 25, 50, 80, and 100 mg-N/L) and photocatalyst dosages (0.1, 0.5, 1.0, and 2.0 g). The NO_3^- removal efficiency of both photocatalysts was 98.96-99.98%, and the catalytic selectivity products were nitrogen gas (N_2), nitrite (NO_2^-), and NH_4^+. Of the two photocatalysts under comparable experimental conditions, 1.0%Ag-TiO_2 provided better NO_3^- removal efficiency. For both photocatalysts, the remaining NH_4^+ was predominantly determined by $[NO_3^-]_0$; higher $[NO_3^-]_0$ led to higher NH_4^+. Multiple linear regression analysis confirmed the dominant role of $[NO_3^-]_0$ in the remaining NH_4^+. The photocatalyst dosage could play an essential role in limiting NH_4^+ in the treated wastewater, with large variation in $[NO_3^-]_0$ from different sources.

1. Introduction

Photocatalytic reduction is an effective technology for removal of nitrate (NO_3^-) in wastewater. The major disadvantage of this process is the ammonium (NH_4^+), an undesirable by-product, remaining at the end. Many researchers studied NO_3^- removal efficiency and the NO_3^- conversion selectivity [1–3]. There are also studies on the influencing factors on the remaining NH_4^+, which investigated the relationships between remaining NH_4^+ and those influencing factors in the process.

Previous studies demonstrated that high efficiency nitrate removal by photocatalytic reduction with low remaining $[NH_4^+]$ could be achieved by silver- (Ag-) doped TiO_2 nanoparticles under high-performance light sources (i.e., high-pressure Hg lamps and xenon lamps) [4–6]. However, those light sources have disadvantages that include high energy consumption, potential human health hazard, and generating high heat [7, 8]. For those reasons, the UVA light bulb is chosen for this process because it overcomes those disadvantages and is powerful enough for this process [9–11].

The influencing factors of the photocatalytic selectivity of NO_3^- conversion include initial nitrate concentration ($[NO_3^-]_0$), light source intensity, type of photocatalyst, type of dopant, and quantity of photocatalyst dosage [4, 12, 13]. Evidence shows that manipulating the photocatalytic selectivity of photocatalytic reduction helps limit environmentally harmful compounds, particularly NH_4^+ [14, 15]. NH_4^+ is

harmful to aquatic life once in the natural waterways where it converts into ammonia (NH_3). According to the United States Environmental Protection Agency (US EPA), the upper safety limit of total ammonia nitrogen (NH_3-N) is 17 mg-N/L (1-hour average) and 1.9 mg-N/L (30-day rolling average) at pH 7.0 and 20°C for acute and chronic criteria, respectively [16]. The reported total ammonia concentrations in treated wastewater from photocatalytic reduction vary between 0.07 and 57.8 mg-N/L [4, 17–22].

Doping of silver (Ag^+) on photocatalysts, especially TiO_2, to improve the photocatalytic performance was a common practice. Previous studies applied 0.1%-7.0% Ag^+ loading on TiO_2 photocatalysts and found that 1% Ag^+ was the most optimum dose to enhance the photocatalytic NO_3^- reduction activity [23–25].

This research investigated the effects of initial nitrate concentrations ($[NO_3^-]_0$) and photocatalyst dosages on NO_3^- removal efficiency in synthetic wastewater using photocatalytic reduction. The experiments were carried out under various $[NO_3^-]_0$ (10, 25, 50, 80, and 100 mg-N/L) and photocatalyst dosages (0.1, 0.5, 1.0, and 2.0 g) under UVA irradiation as light source for photocatalytic nitrate reduction. The experimental photocatalysts were TiO_2 and 1.0%Ag-TiO_2 nanoparticle as photocatalysts [21]. The catalytic selectivity of NO_3^- conversion was also determined, and the actual concentrations of NH_4^+ under different experimental NO_3^- removal conditions were compared. Multiple linear regression was performed to characterize the relationship between the remaining NH_4^+ and $[NO_3^-]_0$ and photocatalyst dosages. Essentially, the novelty of this research lies in the use of TiO_2 nanopowder as photocatalyst, as opposed to commercial-grade TiO_2. By comparison, TiO_2 nanopowder possesses larger surface area for adsorption and reaction. Another research novelty is the systematical use of various $[NO_3^-]_0$ and photocatalyst dosages, unlike previous researches which experimented with specific $[NO_3^-]_0$ and photocatalyst dosages.

2. Materials and Methodology

2.1. Ag-TiO_2 Photocatalyst Preparation and Characteristics. In this research, 1.0%Ag-TiO_2 photocatalyst was prepared by composite colloid deposition under alkaline condition, following Doudrick et al. [4, 9] with minor modifications. In the experiment, 12 g of TiO_2 nanopowder was dispersed in 500 mL deionized water and purged with nitrogen gas (N_2) for 30 min to remove O_2. After degassing, 8 mL of methanol was added and stirred prior to adding NaOH to adjust pH of the mixture to 12-13. Afterward, 1.0%$AgNO_3$ (*w*/*v*; Fluka) was added and stirred in the dark for 30 min before irradiation with UVA (800 μW/cm^2) for 1 h at room temperature.

The mixture was then centrifuged at 200 rpm for 2 min to settle the powder, and the supernatant was discarded. Deionized water was added to wash the powder. It was then stirred and centrifuged. The process was repeated until the mixture pH was 7. The washed powder was oven dried at 103°C for 24 h and calcined at 450°C for 1 h for Ag-TiO_2 photocatalyst in the form of dried light purple powder.

The experimental TiO_2 nanopowder was of 15 nm in particle size and 99.5% anatase crystalline phase (US Research Nanomaterials, Inc., USA). The composition and specific surface area of dose photocatalysts were characterized by transmission electron microscopy (TEM, JEM-1400 TEM instrument) and X-ray fluorescence spectrometer (XRF; Bruker model S8 Tiger), Brunauer, Emmett and Teller (BET) analyzer (BELSORP-max Bel Japan Inc.).

2.2. Photocatalytic Reduction for NO_3^- Removal. The photocatalytic reduction to remove nitrate (NO_3^-) was carried out using TiO_2 and Ag-TiO_2 photocatalysts in 125 mL cylindrical borosilicate glass photoreactor. Figure 1 illustrates the schematic of experimental photocatalytic reduction for NO_3^- removal. Synthetic NO_3^- wastewater of variable initial nitrate concentrations was prepared by dissolving potassium nitrate (KNO_3 > 99%, Fluka) in deionized water. The initial nitrate concentration ($[NO_3^-]_0$) varied between 10, 25, 50, 80, and 100 mg-N/L.

The photoreactor was filled with 100 mL synthetic wastewater of varying $[NO_3^-]_0$ and 58 mM of formic acid (FA) as hole scavenger, with the mixture pH ranging from 2.28 to 2.42. TiO_2 and Ag-TiO_2 photocatalysts of varying dosages were independently added into the photoreactor. The photocatalyst dosage was varied from 0.1, 0.5, 1.0, and 2.0 g. The photoreactor condition was anaerobic by purging with N_2 for 30 min to remove dissolved oxygen (DO) in the synthetic wastewater.

Prior to UVA irradiation, samples were drawn for initial measurement of pH, DO, $[NH_4^+]$, $[NO_2^-]$, and $[NO_3^-]$. The samples were subsequently irradiated with two UVA light bulbs (300 W, Osram) for 6 h. The UVA light bulbs were located on either side of the photoreactor vessel at a distance of 20 cm. The UVA intensity in the photoreactor vessel was 800 μW/cm^2 on average. The concentrations of NO_3^- and by-products ($[NO_2^-]$ and $[NH_4^+]$) relative to reaction time were periodically measured throughout the experiment, while pH and DO were measured at the beginning and at termination (at 360 min). The concentrations of NO_3^-, NO_2^-, and NH_4^+ in the synthesis wastewater were determined using ion chromatography instrument with chemical suppression (Metrohm 882 Compact IC Plus). Nitrogen gas (N_2) was calculated by the mass balance of nitrogen of the photocatalytic reduction process.

To verify the experiment, photocatalytic reduction was also carried out under three control conditions: (1) in the absence of photocatalyst but with UVA irradiation; (2) with Ag-TiO_2 photocatalyst of varying dosages but without UVA irradiation; and (3) with TiO_2 photocatalysts of varying dosages but without UVA irradiation. The measured $[NO_3^-]$, $[NO_2^-]$, and $[NH_4^+]$ of photocatalytic reduction using Ag-TiO_2 and TiO_2 photocatalysts irradiated with UVA were subsequently compared against the controls.

2.3. Selectivity of Photocatalytic Reduction for NO_3^- Removal. The NO_3^- removal efficiency of photocatalytic reduction (η) and the catalytic selectivity (S) of NO_3^- into NH_4^+, NO_2^-, and N_2 (denoted by $S_{NH_4^+}$, $S_{NO_2^-}$, and S_{N_2}) [21, 26] are

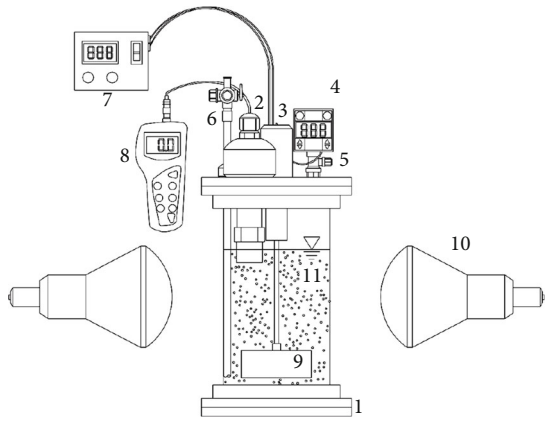

Figure 1: Schematic of photoreactor for nitrate removal.

mathematically expressed in the following equations.

$$\eta = \frac{[NO_3^-]_0 - [NO_3^-]_t}{[NO_3^-]_0} \times 100, \quad (1)$$

$$\%S_{NO_2^-} = \frac{[NO_2^-]_t}{[NO_3^-]_0 - [NO_3^-]_t} \times 100, \quad (2)$$

$$\%S_{NH_4^+} = \frac{[NH_4^+]_t}{[NO_3^-]_0 - [NO_3^-]_t} \times 100, \quad (3)$$

$$\%S_{N_2} = \frac{[NO_3^-]_0 - [NO_3^-]_t - [NO_2^-]_t - [NH_4^+]_t}{[NO_3^-]_0 - [NO_3^-]_t} \times 100, \quad (4)$$

where $[X]_0$ is the initial concentration of X and $[X]_t$ is the concentration of X at time t.

3. Results and Discussion

3.1. Ag-TiO_2 Nanopowder Photocatalyst Characteristics. The results of transmission electron microscopy were used to examine the particle size and morphology of Ag nanoparticles on TiO_2 as well as the lattice information of both photocatalysts investigated by XRF. In comparison, the TEM image of nano-TiO_2 and nano-Ag-TiO_2 photocatalysts (Figure 2) showed a similar particle size and morphology with average particle size (in diameter) of approximately 15 nm (as the result of the average TiO_2 particle size before Ag doping). The results of the TEM analysis were not clearly distinguishable in terms of particle size and morphology although it was reported that Ag doping would slightly decrease the particle size of the larger TiO_2 powders [27].

The XRF patterns of TiO_2 and 1.0%Ag-TiO_2 nanopowder photocatalysts showed strong peaks of Ti, as shown in Figure 3. The XRF pattern of 1.0%Ag-TiO_2 photocatalyst indicated that Ag^+ dopant was effectively doped onto TiO_2 which is the same with the theoretical adding. The Ag dopant in Ag-TiO_2 phase was 0.99% for theoretical doping of 1.0% (Table 1). It was confirmed that Ag was effectively deposited on the surface of TiO_2 nanopowder. Specifically, Ag^+ ions were adsorbed onto the crystal structure of TiO_2 and subsequently formed Ag-TiO_2 [28, 29].

The BET specific surface areas of TiO_2 and 1.0%Ag-TiO_2 nanopowder photocatalysts were 1.164×10^2 and 1.124×10^2 m^2/g, and the corresponding pore volumes were 4.727×10^{-7} and 3.951×10^{-7} m^3/g. It was found that the specific surface area and pore volume of Ag-TiO_2 were decreased after doping. The findings were consistent with previous studies which doped TiO_2 nanopowder photocatalysts with varying dopants [4, 30, 31].

The slightly decreased BET surface areas and pore volume were due to the interference of Ag dopant on the formation of anatase crystallization [32, 33], and a marked influence on the microstructures was exhibited by calcination temperature [34]. However, the advantage of metal doping on semiconductor particles, Ag-TiO_2, was the prevention of recombination between electron and hole by trapping the electron on the metal surface resulting in increasing the lifetime of electron in conduction band, thus enhancing the efficiency of photocatalytic nitrate reduction [34].

3.2. NO_3^- Removal Using Photocatalytic Reduction. The NO_3^- removal efficiency (η) of photocatalytic reduction using TiO_2 and 1.0%Ag-TiO_2 photocatalysts under variable initial NO_3^- concentrations ($[NO_3^-]_0$; 10, 25, 50, 80, and 100 mg-N/L) and TiO_2 and 1.0%Ag-TiO_2 dosages (0.1, 0.5, 1.0, and 2.0 g) was determined by equation (1).

Table 2 tabulates the NO_3^- removal efficiency, nitrate concentration at termination ($[NO_3^-]_t$), ammonium ion selectivity ($\%S_{NH_4^+}$), and actual ammonium ion concentration ($[NH_4^+]_a$) of photocatalytic reduction under various $[NO_3^-]_0$ using TiO_2 and 1.0%Ag-TiO_2 photocatalysts. The NO_3^- removal efficiency of TiO_2 and 1.0%Ag-TiO_2 photocatalysts was 98.96-99.98%. The NO_3^- removal efficiency increased with the increase in photocatalyst dosage as the surface area for adsorption and reaction increased.

The ammonium ion selectivity ($S_{NH_4^+}$) and actual ammonium ion concentration ($[NH_4^+]_a$) increased with the increase in photocatalyst dosage for both TiO_2 and 1.0% Ag-TiO_2 photocatalysts. In addition, the initial nitrate concentration and $[NH_4^+]_a$ were positively correlated. In other words, low $[NO_3^-]_0$ resulted in low $[NH_4^+]_a$ and vice versa. Moreover,

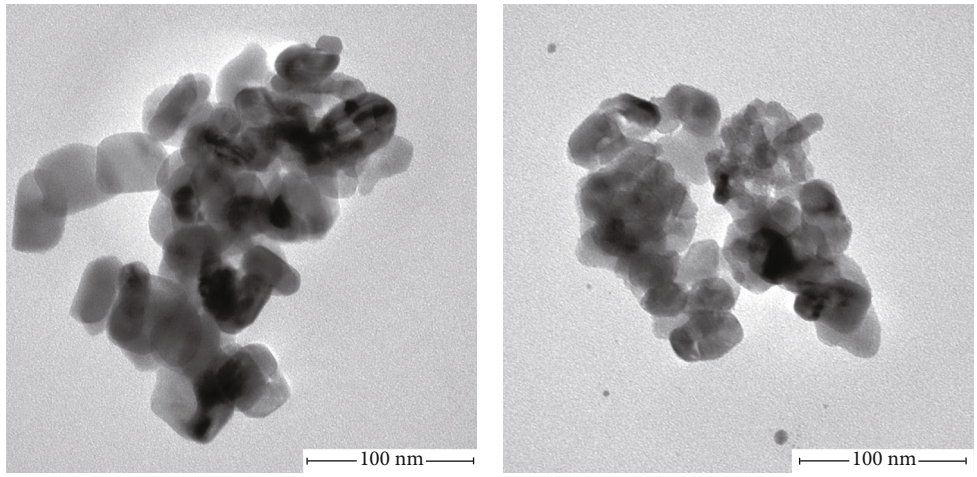

(a) TiO_2 (b) Ag-TiO_2

Figure 2: TEM image of (a) TiO_2 photocatalyst and (b) 1.0%Ag-TiO_2 photocatalyst.

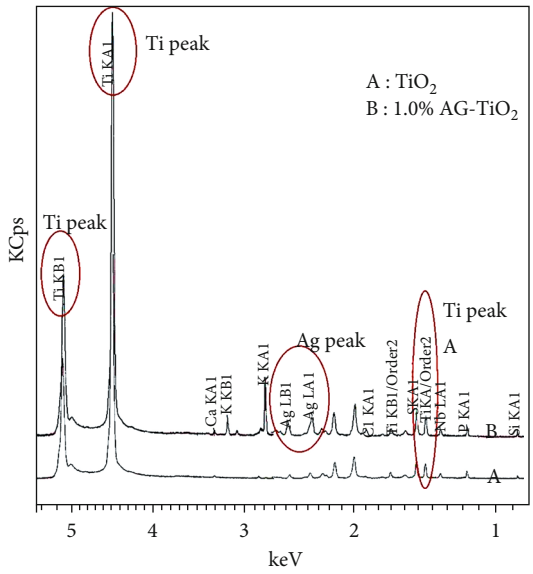

Figure 3: The XRF patterns of TiO_2 and 1.0%Ag-TiO_2 nanopowder photocatalysts.

$[NH_4^+]_a$ of 1.0% Ag-TiO_2 photocatalyst was higher than that of TiO_2 photocatalyst under all experimental conditions.

The NO_3^- reduction in photocatalytic process was a stepwise mechanism. When the photoinduced electrons (e^-) in valence band were excited onto conduction band, holes (h^+) appeared at valence band. This process was called electron-hole pairs photogeneration [32] (equation (5)). The photogenerated holes consumed $HCOO^-$, and $CO_2^{\cdot-}$ was generated [35] (equation (6)). The $CO_2^{\cdot-}$ is a strong reducing agent to reduce NO_3^- to either NH_4^+ or N_2 (equations (7)–(12)), in which nitrite (NO_2^-) was an intermediate product. The results of NO_2^-, NH_4^+, and N_2 in percent named the selectivity of NO_3^- reduction.

$$TiO_2 + hv \rightarrow e^- + h^+ \quad (5)$$

$$HCOO^- + h^+ \rightarrow H^+ + CO_2^{\cdot-} \quad (6)$$

$$NO_3^- + 2H^+ + 2e^- \rightarrow NO_2^- + H_2O \quad (7)$$

$$2NO_3^- + 12H^+ + 10CO_2^{\cdot-} \rightarrow N_2 + 6H_2O + 10CO_2 \quad (8)$$

$$NO_3^- + 10H^+ + 8CO_2^{\cdot-} \rightarrow NH_4^+ + 3H_2O + 8CO_2 \quad (9)$$

$$NO_2^- + 8H^+ + 6CO_2^{\cdot-} \rightarrow NH_4^+ + 2H_2O + 6CO_2 \quad (10)$$

$$2NO_3^- + 12H^+ + 10e^- \rightarrow N_2 + 6CO_2 \quad (11)$$

$$NO_3^- + 10H_2O + 8e^- \rightarrow NH_4^+ + 3H_2O \quad (12)$$

In the nitrate reduction experiments, 58 mmol of formic acid (FA) was used as a hole scavenger to improve the photocatalytic reduction reaction, while the pH of the solution increased from 2.28-2.42 to 2.41-5.5 due to the consumption of formic acid in the reaction and the generation of $[NH_4^+]$. In addition, the highly efficient conversion of NO_2^- to N_2 was also related to the initial acidity of the solution [36]. This was probably due to the specific absorption properties of NO_3^- and NO_2^- in varying pH solutions. Considering that the point of zero charge of the TiO_2 was 6.25 [37], in acidic solution, TiO_2 surface accumulated a net positive charge due to the increasing fraction of $TiOH_2^+$ sites on the surface and NO_2^- could be quickly adsorbed.

Figure 4 compares the nitrate concentrations of photocatalytic reduction under various $[NO_3^-]_0$ and photocatalytic dosages (TiO_2 and 1.0%Ag-TiO_2) from the start to end. In Figure 4, the NO_3^- removal was positively correlated with photocatalyst dosage due to the surface area effect, independent of photocatalyst type. Although at termination there were not much differences in final NO_3^- removal efficiencies, the NO_3^- removal rates of 1.0%Ag-TiO_2 photocatalyst were faster than those of TiO_2 photocatalyst for the comparable conditions. The faster removal rate of photocatalytic reduction activity was attributable to Ag^+ doping [33, 38]. The loading of TiO_2 with Ag^+ reduced the difference between

Table 1: Composition of TiO_2 and 1.0%Ag-TiO_2 photocatalysts.

Photocatalyst	Composition (%)						BET surface area (m^2/g)	Pore volume (m^3/g)
	TiO_2	Ag	SiO_2	P_2O_5	Nb_2O_5	Other		
TiO_2	96.8	—	0.44	0.15	0.11	2.50	1.164×10^2	4.727×10^{-7}
1.0%Ag-TiO_2	96.1	0.99	0.40	0.17	0.11	2.23	1.124×10^2	3.951×10^{-7}

Table 2: NO_3^- removal efficiency, $[NO_3^-]_t$, $\%S_{NH_4^+}$, and $[NH_4^+]_a$ of photocatalytic reduction using TiO_2 and 1.0%Ag-TiO_2 photocatalysts at termination.

Photocatalyst	$[NO_3^-]_0$ (mg-N/L)	Dosage (g)	NO_3^- removal (%)	$\%S_{NH_4^+}$	$[NH_4^+]_a$ (mg-N/L)	pH_t
TiO_2	10	0.1-2.0	98.96-99.48	25.81-34.00	2.55-3.38	2.41-2.84
	25	0.1-2.0	99.35-99.92	20.53-36.5	5.10-9.12	2.54-3.11
	50	0.1-2.0	99.84-99.92	9.53-26.40	4.76-13.18	2.80-3.61
	80	0.1-2.0	99.85-99.98	16.35-25.55	13.06-20.43	2.9-3.28
	100	0.1-2.0	99.90-99.95	17.13-22.56	17.12-22.55	2.93-3.3
1.0%Ag-TiO_2	10	0.1-2.0	99.60-99.62	19.71-64.09	1.96-6.38	2.50-2.51
	25	0.1-2.0	99.30-99.84	17.59-44.81	4.39-11.19	2.52-2.64
	50	0.1-2.0	99.78-99.90	14.97-45.98	7.47-22.97	2.72-3.03
	80	0.1-2.0	99.85-99.94	19.20-38.15	15.33-30.50	3.00-4.02
	100	0.1-2.0	99.82-99.96	16.12-38.10	16.09-38.10	3.06-5.50

Note: $\%S_{NH_4^+}$ is NH_4^+ selectivity (%), $[NH_4^+]_a$ is actual $[NH_4^+]$, and pH_t is pH at the end.

energy levels of the valence and conduction bands, resulting in the extension of light absorption wavelength into the visible light region. Ag^+ also acted as a trap site for excited electrons, giving rise to electron-hole separation. In addition, Ag^+ doping enhanced charge transport, prolonged the lifetime of electron-hole pairs, and reduced the charge recombination [39–42]. As a result, Ag^+ could be adopted for photocatalytic reduction process to improve NO_3^- removal.

Figure 5 illustrates the catalytic selectivity (%) of photocatalytic reduction using TiO_2 and 1.0%Ag-TiO_2 photocatalysts in which NO_3^- was transformed into NO_2^-, NH_4^+, and N_2. The results showed that overall N_2 accounted for the largest proportions of NO_3^- by-products, followed by NH_4^+ and NO_2^-.

In Figure 5, the photocatalyst types (TiO_2 and 1.0%Ag-TiO_2) and dosage played a role in the selectivity of the photocatalytic reduction scheme. This showed that the Ag dopant enhanced the photocatalytic reduction activity, and both the activity and $[NH_4^+]$ increased with 1.0%Ag-TiO_2 dosage increase. However, 1.0%Ag-TiO_2 photocatalyst dosage beyond 0.1 g (i.e., 0.5, 1.0, and 2.0 g) contributed to $[NH_4^+]$ in the treated wastewater exceeding that of TiO_2 photocatalyst (Table 2). NH_4^+ is harmful to aquatic life once in the natural waterways where it converts into NH_3.

The initial nitrate concentrations also played a role in $[NH_4^+]$ in the treated wastewater, independent of photocatalyst type (TiO_2 and 1.0%Ag-TiO_2). Specifically, higher $[NO_3^-]_0$ resulted in higher $[NH_4^+]$. Given 0.1 g of either TiO_2 or 1.0%Ag-TiO_2 photocatalyst, $[NH_4^+]$ was 1.96-16.09 mg-N/L, independent of $[NO_3^-]_0$. Assuming complete NH_4^+-to-NH_3 conversion, these were equivalent to 1.96-16.09 mg-N/L total ammonia nitrogen (NH_3-N), which is below 17 mg-N/L NH_3-N of the US EPA [16]. Meanwhile, the nitrate concentrations of the three control conditions (i.e., the controls) remained unchanged at the end of the experiment.

In Figure 5, the catalytic selectivity of NO_3^- into NO_2^- could also be observed. The remaining nitrite concentrations ($[NO_2^-]$) were negligible as NO_2^- was converted into NH_4^+ and N_2 during the photocatalytic reduction process [43].

To comparatively investigate the effect of initial nitrate concentration and photocatalyst dosage on the concentration of ammonium ion, the relationships between $[NH_4^+]$ and $[NO_3^-]_0$ and photocatalyst dosage (TiO_2 and 1.0%Ag-TiO_2) were established by using statistical multiple linear regression. $[NH_4^+]$, $[NO_3^-]_0$, and photocatalyst dosage are denoted by Y, X_1, and X_2, respectively. The multiple linear regression was expressed in equation (13), and Table 3 tabulates the regression results.

$$Y = b + \beta_1 X_1 + \beta_2 X_2 + \cdots + \varepsilon, \tag{13}$$

where b is the linear regression constant, β is the linear regression coefficient, and ε is the error constant.

In Table 3, β of the initial nitrate concentration ($[NO_3^-]_0$) was, respectively, 0.925 and 0.838 for TiO_2 and 1.0%Ag-TiO_2 photocatalysts ($p < 0.001$), indicating that $[NO_3^-]_0$ played the dominant role in NO_3^- removal efficiency and the remaining NH_4^+. Meanwhile, β of photocatalyst dosage was 0.407 and 0.288 for 1.0%Ag-TiO_2 and TiO_2 photocatalysts, suggesting that the photocatalyst dosage had considerably less effect on the remaining NH_4^+.

In reality, $[NO_3^-]_0$ varies from area to area. Given diverse $[NO_3^-]_0$, it is operationally practical to vary the

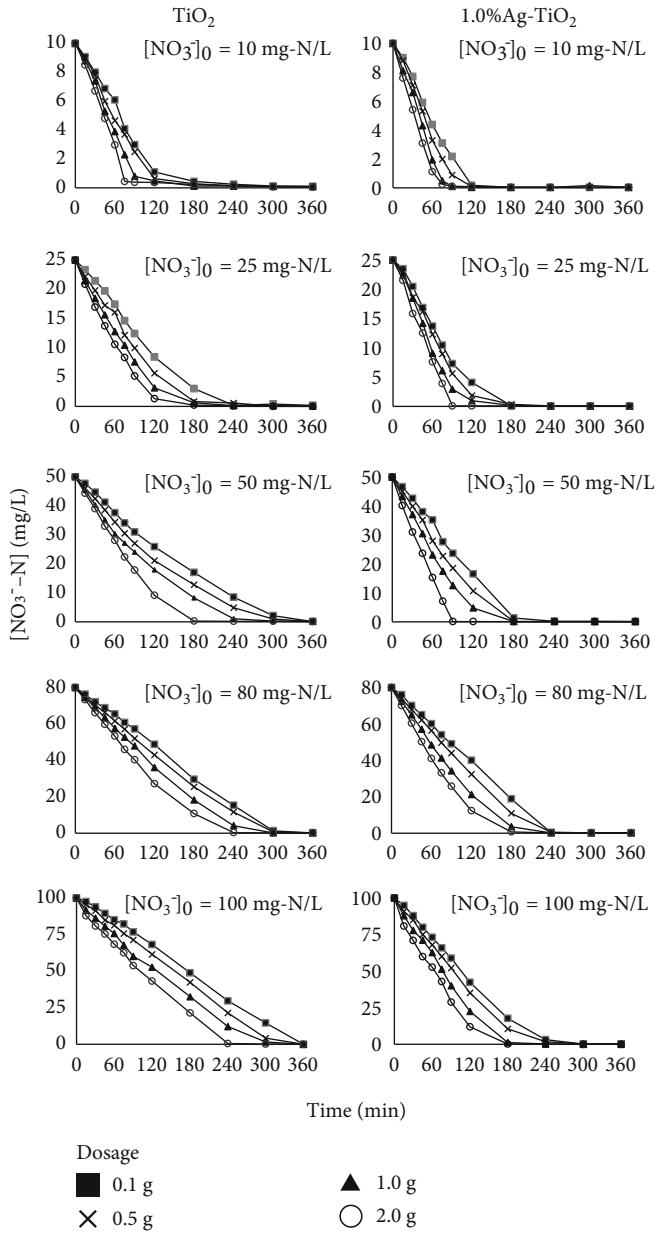

Figure 4: The concentrations of NO_3^- of the photocatalytic reduction scheme under various $[NO_3^-]_0$ and TiO_2 and 1.0%Ag-TiO_2 dosages.

photocatalyst dosage in the photocatalytic reduction scheme. Based on the experimental results, 0.1 g of Ag-TiO_2 photocatalyst is advisable due to efficient removal of NO_3^- (Figure 3).

To facilitate estimation of the remaining $[NH_4^+]$ in treated wastewater using photocatalytic reduction, the multiregression prediction equations of the theoretical remaining ammonium ion ($[NH_4^+]_T$), as a function of $[NO_3^-]_0$ and photocatalyst dosage, are expressed in equations (14) and (15), respectively.

The prediction equation for TiO_2 photocatalyst is

$$[NH_4^+]_T = -1.489 + 0.185[NO_3^-]_0 + 2.698\text{dosage}. \quad (14)$$

The prediction equation for 1.0%Ag-TiO_2 photocatalyst is

$$[NH_4^+]_T = -3.744 + 0.274[NO_3^-]_0 + 6.064\text{dosage}. \quad (15)$$

The relationships between $[NH_4^+]_T$, $[NO_3^-]$, and photocatalyst dosage, as shown in equations (7) and (8), could be further applied to estimate the remaining $[NH_4^+]$ under various $[NO_3^-]_0$ and photocatalyst dosages.

4. Conclusion

This research investigated the NO_3^- removal efficiency of photocatalytic reduction process under various $[NO_3^-]_0$ (10,

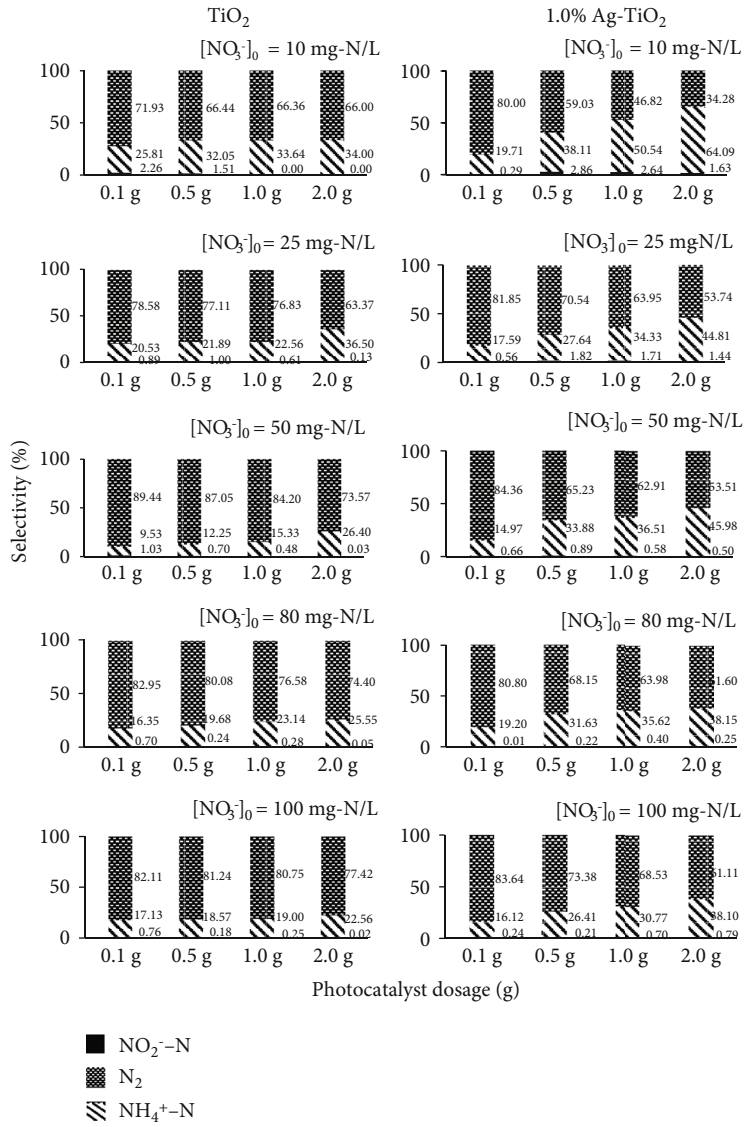

Figure 5: The catalytic selectivity of the photocatalytic reduction scheme under various $[NO_3^-]_0$ and TiO_2 and 1.0%Ag-TiO_2 dosages.

Table 3: Results of multiple linear regression analysis.

Photocatalyst	Independent variables	b	β	t value	p value
TiO_2	$[NO_3^-]_0$	6.879	0.925	15.395	0.000
	Dosage	0.184	0.288	4.787	0.000
	Constant	-1.489		-1.643	0.119
$R = 0.969$, $R^2 = 0.939$, $F = 129.955$, and p value < 0.001.					
1.0%Ag-TiO_2	$[NO_3^-]_0$	0.274	0.838	11.96	0.000
	Dosage	6.064	0.407	5.63	0.000
	Constant	-3.744		-2.16	0.045
$R = 0.955$, $R^2 = 0.911$, $F = 87.30$, and p value < 0.001.					

25, 50, 80, and 100 mg-N/L) and photocatalyst dosages (0.1, 0.5, 1.0, and 2.0 g) using nanoparticle TiO_2 and 1.0%Ag-TiO_2 photocatalysts under UVA. The NO_3^- removal efficiency of both photocatalysts under experimental $[NO_3^-]_0$ and photocatalyst dosages was between 98.96 and 99.98%. The catalytic selectivity products were NH_4^+, NO_2^-, and N_2, with N_2 accounting for a significant proportion of the selectivity. The doping of TiO_2 with Ag^+ improved the removal efficiency of NO_3^-. It was found that $[NO_3^-]_0$ played a more important role in the remaining NH_4^+ than the photocatalyst dosage. Specifically, higher $[NO_3^-]_0$ led to higher $[NH_4^+]$ in the treated wastewater. Multiple linear regression analysis confirmed the dominant role of $[NO_3^-]_0$ in the remaining NH_4^+.

Data Availability

The analysis data used to support the findings of this study are included within the supplementary information file(s).

Conflicts of Interest

The author(s) declare(s) that they have no conflicts of interest.

Acknowledgments

The authors would like to express sincere gratitude to the Faculty of Engineering, Kasetsart University, Thailand, for the technical support.

References

[1] N. Tong, Y. Wang, Y. Liu et al., "PdSn/NiO/NaTaO3:La for photocatalytic ammonia synthesis by reduction of NO3− with formic acid in aqueous solution," *Journal of Catalysis*, vol. 361, pp. 303–312, 2018.

[2] Y. A. Shaban, A. A. El Maradny, and R. K. Al Farawati, "Photocatalytic reduction of nitrate in seawater using C/TiO_2 nanoparticles," *Journal of Photochemistry and Photobiology A: Chemistry*, vol. 328, pp. 114–121, 2016.

[3] D. Sun, W. Yang, L. Zhou, W. Sun, Q. Li, and J. K. Shang, "The selective deposition of silver nanoparticles onto {1 0 1} facets of $_{TiO\ 2}$ nanocrystals with co-exposed {0 0 1}/{1 0 1} facets, and their enhanced photocatalytic reduction of aqueous nitrate under simulated solar illumination," *Applied Catalysis B: Environmental*, vol. 182, pp. 85–93, 2016.

[4] K. Doudrick, T. Yang, K. Hristovski, and P. Westerhoff, "Photocatalytic nitrate reduction in water: managing the hole scavenger and reaction by-product selectivity," *Applied Catalysis B: Environmental*, vol. 136-137, pp. 40–47, 2013.

[5] R. Lucchetti, L. Onotri, L. Clarizia et al., "Removal of nitrate and simultaneous hydrogen generation through photocatalytic reforming of glycerol over "in situ" prepared zero-valent nano copper/P25," *Applied Catalysis B: Environmental*, vol. 202, pp. 539–549, 2017.

[6] E. Bahadori, A. Tripodi, G. Ramis, and I. Rossetti, "Semi-batch photocatalytic reduction of nitrates: role of process conditions and co-catalysts," *ChemCatChem*, vol. 11, no. 18, pp. 4642–4652, 2019.

[7] Z. W. Lipsky and G. K. German, "Ultraviolet light degrades the mechanical and structural properties of human stratum corneum," *Journal of the Mechanical Behavior of Biomedical Materials*, vol. 100, article 103391, 2019.

[8] T. F. Anderson, "Artificial light sources," *Dermatologic Clinics*, vol. 4, no. 2, pp. 203–215, 1986.

[9] T. Rojviroon and S. Sirivithayapakorn, "E. coliBacteriostatic action using TiO2Photocatalytic reactions," *International Journal of Photoenergy*, vol. 2018, 12 pages, 2018.

[10] T. Rojviroon, O. Rojviroon, and S. Sirivithayapakorn, "Photocatalytic decolourisation of dyes using TiO2thin film photocatalysts," *Surface Engineering*, vol. 32, no. 8, pp. 562–569, 2016.

[11] M. Long, J. Wang, H. Zhuang, Y. Zhang, H. Wu, and J. Zhang, "Performance and mechanism of standard nano-TiO_2 (P-25) in photocatalytic disinfection of foodborne microorganisms – Salmonella typhimurium and Listeria monocytogenes," *Food Control*, vol. 39, pp. 68–74, 2014.

[12] J. Yuan, E. Wang, Y. Chen, W. Yang, J. Yao, and Y. Cao, "Doping mode, band structure and photocatalytic mechanism of B–N-codoped TiO_2," *Applied Surface Science*, vol. 257, no. 16, pp. 7335–7342, 2011.

[13] K. Nakata and A. Fujishima, "TiO_2 photocatalysis: design and applications," *Journal of Photochemistry and Photobiology C: Photochemistry Reviews*, vol. 13, no. 3, pp. 169–189, 2012.

[14] F. Zhang, R. Jin, J. Chen et al., "High photocatalytic activity and selectivity for nitrogen in nitrate reduction on $_{Ag/TiO}$ catalyst with fine silver clusters," *Journal of Catalysis*, vol. 232, no. 2, pp. 424–431, 2005.

[15] H. O. N. Tugaoen, S. Garcia-Segura, K. Hristovski, and P. Westerhoff, "Challenges in photocatalytic reduction of nitrate as a water treatment technology," *Science of The Total Environment*, vol. 599-600, pp. 1524–1551, 2017.

[16] EPA, *Final aquatic life ambient water quality criteria for ammonia-freshwater*, 2013, https://www.federalregister.gov/documents/2013/08/22/2013-20307/final-aquatic-life-ambient-water-quality-criteria-for-ammonia-freshwater-2013.

[17] L. Li, Z. Xu, F. Liu et al., "Photocatalytic nitrate reduction over Pt–Cu/TiO_2 catalysts with benzene as hole scavenger," *Journal of Photochemistry and Photobiology A: Chemistry*, vol. 212, no. 2-3, pp. 113–121, 2010.

[18] J. Sá, C. A. Agüera, S. Gross, and J. A. Anderson, "Photocatalytic nitrate reduction over metal modified TiO_2," *Applied Catalysis B: Environmental*, vol. 85, no. 3-4, pp. 192–200, 2009.

[19] T. Yang, K. Doudrick, and P. Westerhoff, "Photocatalytic reduction of nitrate using titanium dioxide for regeneration of ion exchange brine," *Water Research*, vol. 47, no. 3, pp. 1299–1307, 2013.

[20] K. Kobwittaya and S. Sirivithayapakorn, "Photocatalytic reduction of nitrate over TiO_2 and Ag-modified TiO_2," *Journal of Saudi Chemical Society*, vol. 18, no. 4, pp. 291–298, 2014.

[21] J. M. A. Freire, M. A. F. Matos, D. S. Abreu et al., "Nitrate photocatalytic reduction on TiO_2: metal loaded, synthesis and anions effect„" *Journal of Environmental Chemical Engineering*, vol. 8, no. 4, article 103844, 2020.

[22] S. Cao, R. Du, Y. Peng, B. Li, and S. Wang, "Novel two stage partial denitrification (PD)-Anammox process for tertiary nitrogen removal from low carbon/nitrogen (C/N) municipal sewage," *Chemical Engineering Journal*, vol. 362, pp. 107–115, 2019.

[23] L. M. Santos, W. A. Machado, M. D. França et al., "Structural characterization of Ag-doped TiO_2 with enhanced photocatalytic activity," *RSC Advances*, vol. 5, no. 125, pp. 103752–103759, 2015.

[24] S. Krejčíková, L. Matějová, K. Kočí et al., "Preparation and characterization of Ag-doped crystalline titania for photocatalysis applications," *Applied Catalysis B: Environmental*, vol. 111-112, pp. 119–125, 2012.

[25] K. Gupta, R. P. Singh, A. Pandey, and A. Pandey, "Photocatalytic antibacterial performance of TiO_2 and Ag-doped TiO_2 against S. aureus. P. aeruginosa and E. coli," *Beilstein Journal of Nanotechnology*, vol. 4, pp. 345–351, 2013.

[26] N. Krasae and K. Wantala, "Enhanced nitrogen selectivity for nitrate reduction on Cu–nZVI by TiO_2 photocatalysts under UV irradiation," *Applied Surface Science*, vol. 380, pp. 309–317, 2016.

[27] M. Ahamed, M. A. M. Khan, M. J. Akhtar, H. A. Alhadlaq, and A. Alshamsan, "Ag-doping regulates the cytotoxicity of TiO_2 nanoparticles via oxidative stress in human cancer cells," *Scientific Reports*, vol. 7, no. 1, p. 17662, 2017.

[28] Y. Luo, S. Yu, B. Li et al., "Synthesis of (Ag,F)-modified anatase TiO2nanosheets and their enhanced photocatalytic activity," *New Journal of Chemistry*, vol. 40, no. 3, pp. 2135–2144, 2016.

[29] R. Saravanan, D. Manoj, J. Qin et al., "Mechanothermal synthesis of Ag/TiO_2 for photocatalytic methyl orange degradation and hydrogen production," *Process Safety and Environmental Protection*, vol. 120, pp. 339–347, 2018.

[30] N. T. Minh and B.-K. Lee, "Feasibility of silver doped TiO_2/-glass fiber photocatalyst under visible irradiation as an indoor air germicide," *International Journal of Environmental Research and Public Health*, vol. 11, pp. 3271–3288, 2014.

[31] L. Lu, G. Wang, Z. Xiong et al., "Enhanced photocatalytic activity under visible light by the synergistic effects of plasmonics and Ti^{3+}-doping at the Ag/TiO2- heterojunction," *Ceramics International*, vol. 46, no. 8, pp. 10667–10677, 2020.

[32] A. Herissan, J. Meichtry, H. Remita, C. Colbeau-Justin, and M. Litter, "Reduction of nitrate by heterogeneous photocatalysis over pure andradiolytically modified TiO_2 samples in the presence of formic acid," *Catalysis Today*, vol. 281, 2016.

[33] L. Elsellami, F. Dappozze, A. Houas, and C. Guillard, "Effect of Ag^+ reduction on the photocatalytic activity of Ag-doped TiO_2," *Superlattices and Microstructures*, vol. 109, pp. 511–518, 2017.

[34] X. F. Lei, X. X. Xue, and H. Yang, "Preparation and characterization of Ag-doped TiO_2 nanomaterials and their photocatalytic reduction of Cr(VI) under visible light," *Applied Surface Science*, vol. 321, pp. 396–403, 2014.

[35] D. Zhang, B. Wang, X. Gong, Z. Yang, and Y. Liu, "Selective reduction of nitrate to nitrogen gas by novel Cu_2O-Cu_0@Fe_0 composite combined with HCOOH under UV radiation," *Chemical Engineering Journal*, vol. 359, pp. 1195–1204, 2019.

[36] W. Gao, R. Jin, J. Chen et al., "Titania-supported bimetallic catalysts for photocatalytic reduction of nitrate," *Catalysis Today*, vol. 90, no. 3-4, pp. 331–336, 2004.

[37] F. Zhang, Y. Pi, J. Cui, Y. Yang, X. Zhang, and N. Guan, "Unexpected selective photocatalytic reduction of nitrite to nitrogen on silver-doped titanium dioxide," *The Journal of Physical Chemistry C*, vol. 111, no. 9, pp. 3756–3761, 2007.

[38] S. Parastar, S. Nasseri, S. H. Borji et al., "Application of Ag-doped TiO2nanoparticle prepared by photodeposition method for nitrate photocatalytic removal from aqueous solutions," *Desalination and Water Treatment*, vol. 51, no. 37-39, pp. 7137–7144, 2013.

[39] J. Huang, L. Ding, Y. Xi et al., "Efficient silver modification of TiO_2 nanotubes with enhanced photocatalytic activity," *Solid State Sciences*, vol. 80, pp. 116–122, 2018.

[40] R. Qian, H. Zong, J. Schneider et al., "Charge carrier trapping, recombination and transfer during TiO_2 photocatalysis: an overview," *Catalysis Today*, vol. 335, 2018.

[41] S. Buda, S. Shafie, S. A. Rashid, H. Jaafar, and N. F. M. Sharif, "Enhanced visible light absorption and reduced charge recombination in AgNP plasmonic photoelectrochemical cell," *Results in Physics*, vol. 7, pp. 2311–2316, 2017.

[42] B. Xin, L. Jing, Z. Ren, B. Wang, and H. Fu, "Effects of simultaneously doped and deposited Ag on the photocatalytic activity and surface states of TiO_2," *The Journal of Physical Chemistry B*, vol. 109, no. 7, pp. 2805–2809, 2005.

[43] G. Tokazhanov, E. Ramazanova, S. Hamid, S. Bae, and W. Lee, "Advances in the catalytic reduction of nitrate by metallic catalysts for high efficiency and N_2 selectivity: a review," *Chemical Engineering Journal*, vol. 384, p. 123252, 2020.